Supplemental Online Content

Tian YE, Di Biase MA, Mosley PE, et al. Evaluation of brain-body health in individuals with common neuropsychiatric disorders. *JAMA Psychiatry*. Published online April 26, 2023. doi:10.1001/jamapsychiatry.2023.0791

eTable 8. Diagnostic codes of generalized anxiety disorder

eTable 9. Diagnostic codes of dementia

This supplemental material has been provided by the authors to give readers additional information about their work.

eMethods

Data and participants

Physical, physiological and blood/urine-derived phenotypes and/or neuroimaging data were integrated across multiple databases and studies. The data included from each study is summarized below.

UK Biobank

The UK Biobank is a large-scale biomedical database and research resource containing genetic, lifestyle and health information from approximately 500,000 participants[1,2]. The UK Biobank has approval from the North West Multi-centre Research Ethics Committee (MREC) to obtain and disseminate data and samples from the participants (http://www.ukbiobank.ac.uk/ethics/). Written informed consent was obtained from all participants. Individuals aged between 37-74 years were recruited in 2006-2010 at 22 assessment centers from across the UK and underwent extensive physical and physiological assessments, blood and urine sample assays, genome-wide genotyping and questionaries. Multimodal brain imaging[2] was collected in 2014-2020 at three mirrored imaging centers located at Manchester, Reading and Newcastle, respectively, in a subset of individuals aged between 45-82 years (n≈49,000).

Individuals with a lifetime diagnosis of one or more common neuropsychiatric disorders, including schizophrenia (n=2,100, 1,184 males), bipolar disorder (n=5,853, 2,696 males), depression (n=81,631, 27,923 males), generalized anxiety disorder (n=11,456, 3,841 males) and dementia (n=6,503, 3,470 males), as well as individuals without any chronic major medical conditions (healthy comparison individuals, HC, n=84,308, 39,255 males) were included in the present study (Project ID 60698). Among them, a total of 18,280 (7,514 males) and 17,185 (7,018 males) individuals had completed T1-weighted and diffusion magnetic resonance brain imaging assessments respectively.

Diagnostic status and medical conditions were obtained through self-report (verbal interview at assessment centers, UK Biobank Field ID: 20002) and health care records (primary care and hospital inpatient) from the UK National Health Services. Specifically, summary inpatient diagnoses (Field IDs: 41270; 41271) coded by distinct ICD (International Classification of Diseases and Related Health Problems)-9 and/or ICD-10 (July 2020 release) and the primary care data (Read Codes, Field ID: 42040) in relation to clinical events of diagnoses (November 2020 release) were used in this study. Diagnoses coded in Read were mapped to corresponding ICD codes according to the lookup table ('all_lkps_maps_v2.xlsx') (https://biobank.ndph.ox.ac.uk/showcase/showcase/auxdata/primarycare_codings.zip). Of note, each disorder group was defined broadly with all causes and subtypes included. For example, the dementia group included self-reported dementia/Alzheimer's disease/cognitive impairment (UK Biobank code: 1263); health care recorded ICD-9 and/or 10 coded various types of dementia (e.g., Alzheimer's diseases, vascular dementia, dementia in other diseases classified elsewhere). eTables 5-9 list diagnostic codes related to each of the five disease categories. In addition to the interview-based self-report and health care records, individuals with a lifetime diagnosis of bipolar disorder, depression and generalized anxiety disorder identified based on DSM (Diagnosis and Statistical Manual of Mental Disorders)-IV criteria using the online Mental Health Questionnaire[3,4] were also included. Individuals who had more

than one diagnosis were grouped into multiple disorder groups. The majority of individuals had a single neuropsychiatric diagnosis (77,185/91,636=84.23%) and the proportion of individuals comorbid with 2 to 5 neuropsychiatric conditions was 14.26% (n=13,070), 1.42% (n=1,305), 0.08% (n=74) and 0.002% (n=2), respectively. Pairwise comorbidity is most common for depression and generalized anxiety disorder (9,166/13,070=70.13%), followed by depression and bipolar disorder (3,475/13,070, 26.59%), depression and schizophrenia (1,119/13,070=8.56%), bipolar disorder and generalized anxiety disorder (960/13,070=7.35%), with small comorbidity rates (<5%) observed for other diagnosis pairs. Comorbidity with 3 neuropsychiatric conditions was most common for bipolar disorder, depression and generalized anxiety disorder (803/1,305=61.53%) and followed by schizophrenia, bipolar disorder and depression (254/1,305=19.46%). Other patterns of comorbidity were relatively rare.

Brain phenotypes

Brain gray matter and white matter phenotypes derived from T1-weighted magnetic resonance imaging (MRI) and diffusion MRI (dMRI) were sourced from the UK Biobank[2]. The image processing pipeline, artefact removal, cross-modality and cross-individual image alignment, quality control and phenotype calculation are described in detail elsewhere[5] and also in the UK Biobank brain imaging documentation (https://biobank.ctsu.ox.ac.uk/showcase/showcase/docs/brain_mri.pdf).

Regional gray matter volume and cortical thickness estimates derived from T1-weighted MRI using FreeSurfer 6[6] were used to map brain gray matter health. The Desikan-Killiany atlas[7] was used for cortical parcellation. Regional microstructural measures of white matter tracts including fractional anisotropy (FA) and mean diffusivity (MD) were derived from dMRI using the JHU ICBM-DTI-81 white matter atlas[8]. FA maps were skeletonized and mapped onto Montreal Neurological Institute standard space using tract-based spatial statistics (TBSS)[9]. All regional measures were averaged across the left and right hemispheres, resulting in 76 gray matter (eTable 1) and 54 white matter (eTable 2) phenotypes for further analyses. The same set of MRI-derived gray and white matter phenotypes were derived from the other six consortia studies (where available).

Body phenotypes

Physical, physiological and blood/urine-derived phenotypes known to associate with the function and health status of 7 body systems, including the cardiovascular, pulmonary, musculoskeletal, immune, renal, hepatic and metabolic systems were selected. Phenotypes primarily sourced from the UK Biobank were supplied with the original Field IDs where applicable. Phenotypes secondarily computed include: i) the average handgrip strength across left and right hand; ii) the average heel bone mineral density across left and right heel; iii) the average ankle spacing width across left and right ankle; iv) the total-to-HDL cholesterol ratio; v) the FEV1 (forced expiration volume in 1-second)/FCV (forced vital capacity) ratio; and vi) the waist-hip circumference ratio. This resulted in a total of 73 body phenotypes for further analyses (eTable 3). The original UK Biobank data field IDs of variables were provided where applicable.

ASRB

The Australian Schizophrenia Research Bank (ASRB)[10] is a comprehensive biobank of clinical, neuroimaging and genetic data acquired in individuals with schizophrenia and healthy comparison individuals. The study was approved by the Melbourne Health Human Research Committee (Project ID: 2010.250). All participants provided written informed consent for the analysis of their data. Participants were acquired from five sites in Australia, including Melbourne, Sydney, Brisbane, Perth and Newcastle using identical recruitment and brain MRI acquisition protocols. Diagnoses were confirmed using the Diagnostic Interview for Psychosis. Exclusion criteria included any neurological disorder, history of brain trauma followed by a long period of amnesia (>24 h), intellectual disability of intelligence quotient below 70, current drug or alcohol dependence, as well as electroconvulsive therapy in the past 6 months. The T1-weighted MRI and diffusion MRI of 323 (age range 20-66 years 95 males) individuals with schizophrenia, and 183 (age range 18-66 years, 94 males) healthy comparison individuals were included in the present study. Details of imaging acquisition and pre-processing are described in detail elsewhere[11].

AIBL

the Australian Imaging, Biomarkers and Lifestyle Flagship Study of Ageing (AIBL) (https://aibl.csiro.au/) is a study to discover which biomarkers, cognitive characteristics, and health and lifestyle factors determine subsequent development of symptomatic Alzheimer's Disease. AIBL study methodology has been reported previously[12]. The AIBL study was approved by the institutional ethics committees of Austin Health, St Vincent's Health, Hollywood Private Hospital and Edith Cowan University, and all volunteers gave written informed consent before participating in the study. T1-weighted MRI brain images acquired at baseline assessments for 58 (age range 55-85 years; 23 males) individuals diagnosed with dementia, and 400 (age range 60-92 years, 156 males) healthy comparison individuals were included in this study. AIBL data were acquired from four sites in Australia, including Perth, Sydney, Adelaide and Melbourne. Consistent with the UK Biobank, MRI brain images were processed using FreeSurfer 6, resulting in 76 gray matter phenotypes. AIBL does not have dMRI data.

ADNI

The Alzheimer's Disease NeuroImaging Initiative (http://adni.loni.usc.edu/) was launched in 2003 as a public-private partnership, led by Principal Investigator Michael W. Weiner, MD. The primary goal of ADNI has been to test whether serial magnetic resonance imaging, positron emission tomography, other biological markers, and clinical and neuropsychological assessment can be combined to measure the progression of mild cognitive impairment and early Alzheimer's disease. For up-to-date information, see www.adni-info.org. Details of brain image acquisition can be found elsewhere[13]. As per ADNI protocols, all procedures performed in ADNI studies involving human participants were in accordance with the ethical standards of the institutional and/or national research committee and with the 1964 Helsinki declaration and its later amendments or comparable ethical standards. T1-weighted MRI brain images acquired at baseline assessments across all three phases of ADNI were included, resulting in 205 (age range 55-91 years, 100 males) individuals diagnosed with dementia and 468 (age range 50-95 years, 192 males) healthy comparison individuals. T1-weighted images were processed using FreeSurfer 6. Baseline diffusion MRI brain images acquired at ADNI-GO/ 2 and ADNI 3 were included, resulting in 114 (age range 55-91 years, 73 males) individuals diagnosed with dementia and 471 (age range 50-96 years, 182 males) healthy comparison

individuals. FA and MD maps were computed from the dMRI data using FSL 6 (http://www.fsl.fmrib.ox.au.uk). Head motion and eddy current-induced distortions were corrected using the eddy tool in FSL.

PISA

The Prospective Imaging Study of Ageing: Genes, Brain and Behaviour (PISA)[14] studies the interplay between genetic, epigenetic and environmental factors for dementia, and also aims to identify risk factors that could be modified through intervention (https://www.qimrberghofer.edu.au/study/prospective-imaging-study-of-ageing/). The PISA study protocol has approval from the Human Research Ethics Committees of QIMR Berghofer Medical Research Institute and the University of Queensland. Written informed consent was obtained from all participants. T1-weighted MRI brain images of 31 (age range 51-78 years, 13 males) individuals diagnosed with dementia and 235 (age range 43-82 years, 54 males) healthy comparison individuals were included in this study. T1-weighted images were processed using FreeSurfer 6. Diffusion MRI brain images were available for 32 (age range 43-78 years, 13 males) individuals diagnosed with dementia and 236 (age range 43-82 years, 53 males) healthy comparison individuals. Consistent with as described above, FSL 6 was used to process the dMRI data and the eddy tool of FSL was used to correct head motion and eddy current-induced distortions.

HCP-YA & HCP-Aging

The Human Connectome Project Young Adult (HCP-YA)[15] and the Aging (HCP-A) cohorts[16] comprise the HCP lifespan project (https://www.humanconnectome.org/lifespan-studies). T1-weighted brain MRI images of 1,113 (age range 22-37 years, 507 males) and 709 (36-90 years, 313 males) healthy individuals were sourced from HCP-YA and HCP-A respectively. Diffusion brain MRI images were available for 1,034 (age range 22-37 years, 474 males) and 695 (age range 22-37 years, 309 males) healthy individuals in each dataset. Brain images were processed using the HCP minimal pre-processing pipeline[17]. The HCP datasets were acquired by the WU-Minn HCP consortium with local human research ethics approval and shared with us in accordance with the WU-Minn HCP consortium Open Access and Restricted Data Use Terms. Written informed consent was obtained from all participants.

Brain MRI image quality control

In addition to the quality control and artifact removal performed in each dataset, for all datasets, the quality of the T1-weighted images was further assessed using the Euler number, an index generated by FreeSurfer *recon-all* that measures the topological complexity of a reconstructed cortical surface[18]. Following previous recommendations[19], images with a Euler number less than -217 were deemed poor quality and thus discarded. For diffusion MRI, images with in-scanner head motion residing more than three standard deviations from the median were discarded due to the potential impact of motion on fitting of the diffusion tensor and estimation of fractional anisotropy and mean diffusivity[20]. A summary head motion parameter was computed as the average displacement of each voxel across all volumes (FSL eddy output: eddy_movement_rms). Finally, images with any MRI-derived phenotypes residing more than six standard deviations from the median were discarded from each dataset respectively. This resulted in the final sample as described above.

Data harmonization

Brain imaging-derived phenotypes were harmonized using Combat (https://github.com/Jfortin1/ComBatHarmonization)[21,22], to control for site and scanner variation. Age, sex and diagnostic status were included as biological covariates in the harmonization. Specifically, brain phenotypes were first harmonized within each cohort if brain images were acquired from more than one MRI scanner. This was applied to the UK Biobank (4 scanners), ASRB (5 scanners), AIBL (4 scanners) and ADNI (76 scanners). Of note, the harmonization of gray matter phenotypes within the ADNI cohort was performed in a larger sample, where individuals with mild cognitive decline were also included (n=713), to ensure data from at least 10 individuals were available from each MRI scanner, enabling reliable harmonization. Due to varied acquisition protocols (e.g., the number and/or distribution of diffusion-weighted gradients, angular resolution and scan duration) for ADNI dMRI data, we followed previous work[23], in which FA and MD measures were first harmonized across 8 acquisition protocols using Combat. Linear mixed-effects models were then used to model random effects of scanner nested in dMRI protocol (protocol|scanner). The within-cohort harmonized data were then harmonized across all cohorts, yielding a final set of harmonized brain phenotypes for further analyses.

Normative modeling

The *gamlss* package (version 5.4-3)[24] in R for generalized additive models for local, scale and shape (GAMLSS)[25] was used to establish sex-specific normative references (median and centiles) over the adult lifespan for each brain and body phenotype in healthy individuals combined across cohorts. Cohort differences were modeled as random effects for brain phenotypes. We first evaluated a range of GAMLSS distribution families (n=21) with three or four parameters (i.e., μ, σ, ν, τ)[26]. To determine the best fitting distribution, for each distribution type, we fitted GAMLSS to global brain phenotypes, including mean cortical thickness, total gray matter volume, total cerebrospinal fluid (ventricles) volume, mean FA, as well as representative body phenotype for each body system (handgrip strength, FEV1, systolic blood pressure, C-reactive protein, serum creatine, cholesterol ratio, serum alanine aminotransferase). Of note, evaluation of the best fitting distribution was based on global brain phenotypes because they are likely more reliable and less noisy than regionally specific brain phenotypes. A second order fractional polynomial was used for μ and σ.

The goodness of model fitting was evaluated by i) model stability, i.e., whether a model converges after iterative fitting. We used the default convergence criterion of loglikelihood=0.001 between iterations but increased the maximal iteration cycles from 20 to 100; and ii) the Bayesian Information Criteria (BIC). The optimal model distribution was thus selected as the one with the lowest BIC among converged models. We found that while the optimal model varied across the 11 representative phenotypes, the Box-Cox t distribution generally yielded the lowest BIC compared to other distribution families (eFigure 2). We therefore used GAMLSS with the Box-Cox t distribution to model the age-related phenotypic variation for each phenotype in healthy individuals. Individual variation in each phenotype, denoted with y, was thus modeled such that,

$$
\begin{aligned}
y &= BCT(\,\mu, \sigma, \nu, \tau) \\
\mu &= f_{\mu}^{1}(\text{age}) + f_{\mu}^{2}\,(\text{sex}) + \beta_{\mu} z_{\text{site}} \\
\sigma &= f_{\sigma}(\text{age}), \qquad \nu = \beta_{\nu}, \qquad \tau = \beta_{\tau}\,.
\end{aligned}
$$

In the above model, BCT denotes the Box-Cox t distribution, which is a shifted and truncated version of the t distribution. The distribution was parameterized with four parameters: median/location (μ), centile-based coefficient of variation (σ), skewness (ν) and kutosis (τ).

Normative references ranges (i.e., quantiles) as a function of age and sex were derived from the GAMLSS and then used to estimate standardized phenotypic deviation scores (z-scores)[27,28] for individuals with schizophrenia, bipolar disorder, depression, generalized anxiety disorder and dementia. The z-scores were estimated using quantile randomized residuals[29], whereby the quantiles of the fitted Box-Cox t distribution were mapped onto z-scores of a standard Gaussian distribution.

Deviations scores for healthy individuals were estimated using 10-fold cross-validation. For each 10-fold cross-validation, a GAMLSS model was fitted in individuals comprising 9 folds (training set). The fitted model parameters (μ, σ, ν, τ) were then applied iteratively to the held out set of individuals (test set), resulting in estimated centiles. Phenotypic deviation scores were then computed accordingly as described above. The normality of the distribution of the computed z-scores were evaluated using a two-sided Kolmogorov-Smirnov test.

Estimating organ/system-specific health scores

An organ/system health score (OHS) was estimated for each organ system and for each individual. The OHS is a weighted sum of deviation scores (z-scores) across all phenotypes pertaining to a specific organ system. Phenotype weights were estimated based on the importance of each phenotype toward differentiating healthy individuals from a patient group: i) diagnosed with one or more chronic diseases that primarily affects the organ/system under consideration; and ii) excluding individuals with comorbid psychiatric illness.

For example, for the metabolic system, a logistic regression model was trained to differentiate between healthy comparison individuals and a group of patients with chronic metabolic diseases, including diabetes mellitus (ICD 10 code E10-E14) and/or disorders of lipoprotein metabolism (E78), using phenotypes deviation scores pertaining to the metabolic system. The regression coefficients (phenotype weights) fitted in this logistic regression were then used to compute the metabolic health score for individuals with neuropsychiatric disorders. Individuals comorbid with any of the five neuropsychiatric disorders were not included in the fitting of the logistic regression. This approach was repeatedly applied for all 7 body systems, where the patient group was adjusted to include disease categories most relevant to the system under consideration as outlined in ICD-10. The disease categories selected for each body system are provided in eTable 4. This process resulted in 7 sets of the phenotype weights (i.e., logistic regression coefficients). The overall body health score was computed based on phenotype weights estimated in a combined group of patients diagnosed with chronic diseases affecting multiple body systems. Similarly for the brain, however, health scores computed for a given neuropsychiatric disorder were based on phenotype weights estimated in individuals in the other four groups, to avoid circularity.

More specifically, the organ health score (OHS) for individual $n = 1, \dots, N$ and organ system $k \in$ {cardiovascular, pulmonary, musculoskeletal, immune, renal, hepatic, metabolic, brain}, was given by,

$$OHS(n,k) = -\left(w_0^k + \sum_{j=1}^{J} w_j^k x_j(n)\right)$$

Where w_j^k is the fitted regression coefficient for phenotype $j = 1, \ldots J$ and $x_j(n)$ is the phenotype deviation score (z-score) for the nth individual, as inferred from the GAMLSS. As described above, w_j^k are regression coefficients fitted in a logistic regression differentiating healthy comparison individuals from a group of patients with chronic diseases that primarily affect the kth organ system (see eTable 4 for the list of chronic diseases associated with each organ system). The OHS was multiplied by -1, to ensure that poor organ health is indicated by a lower organ health score across different organ systems. We set $w_0^k = -\sum_{n\in\text{healthy}} \sum_{j=1}^{J} w_j^k x_j(n) \,/H$ to ensure that the distribution of OHS across healthy comparison individuals was necessarily centered at zero, where H is the number of healthy individuals. The center of the OHS distribution would otherwise vary according to the relative proportion of individuals in the patient and healthy comparison groups.

Ten-fold cross-validation was used to compute the OHS for healthy individuals. Specifically, for each 10-fold cross-validation, the regression coefficients (phenotype weights) fitted in the training set (9 folds) were iteratively used to compute the organ health score for the held out set of individuals (test set). Rather than removing individuals with any missing data, an organ-specific missing data handling procedure was used, where the OHS was computed for individuals without any missing entries (e.g., the immune health score was only computed for individuals with no missing entries for all phenotypes comprising the immune system).

Organ health scores are conceptually similar to allostatic load estimation[30]. Indeed, allostatic load and organ health scores include several common phenotypes, such as cholesterol, glycated hemoglobin, systolic and diastolic blood pressure[31,32]. This overlap in phenotypes is consistent with established links between chronic stress and poor organ health. Whereas allostatic load specifically measures the physiological impacts of chronic stress exposure and the effects of "wear and tear"[33], organ health scores focus on characterizing the health and function of specific organs and body systems. Other key differences include benchmarking to normative reference ranges for organ health scores and differences in the way that items are scored [31,32].

Further methodological considerations are worthy of mention. First, organ health is multifaceted, and it is unlikely that a single organ health score will be adequate for all individuals and conditions. Further work is needed to validate the organ health scores developed here in independent community samples. However, validation studies are currently challenging due to the lack of available datasets with the same breadth of brain and body markers as the UK Biobank. Second, as the field evolves, we anticipate that standardized measures of organ health will be established, potentially incorporating specialized markers and non-clinical tests of organ function, such as brain spectroscopy and cardiac diffusion MRI. Finally, many of the markers comprising our health scores are already widely assayed in primary care (e.g., systolic and diastolic blood pressure, glycated hemoglobin, blood lipids), facilitating feasible clinical implementation of organ health scores in this setting.

Diagnostic and transdiagnostic neuropsychiatric disorder classification

Logistic regression models were trained to classify an individual's diagnostic status (schizophrenia, bipolar disorder, depression, generalized anxiety disorder vs healthy comparison individuals) based on phenotypic deviation scores. Using 10-fold cross validation, models were developed for each brain and body system and for each pair of diagnostic (disease vs healthy comparison group) and transdiagnostic (disease vs disease) classifications (eFigure 1D). Classification accuracy was quantified with the area under the receiver operating characteristic curve. Confidence intervals of classification accuracy were estimated by 100 repartitions of 10-fold cross-validation. Regression coefficients estimated from cross-validation iterations were averaged, yielding a consensus representation of feature (phenotype) importance in disease classification.

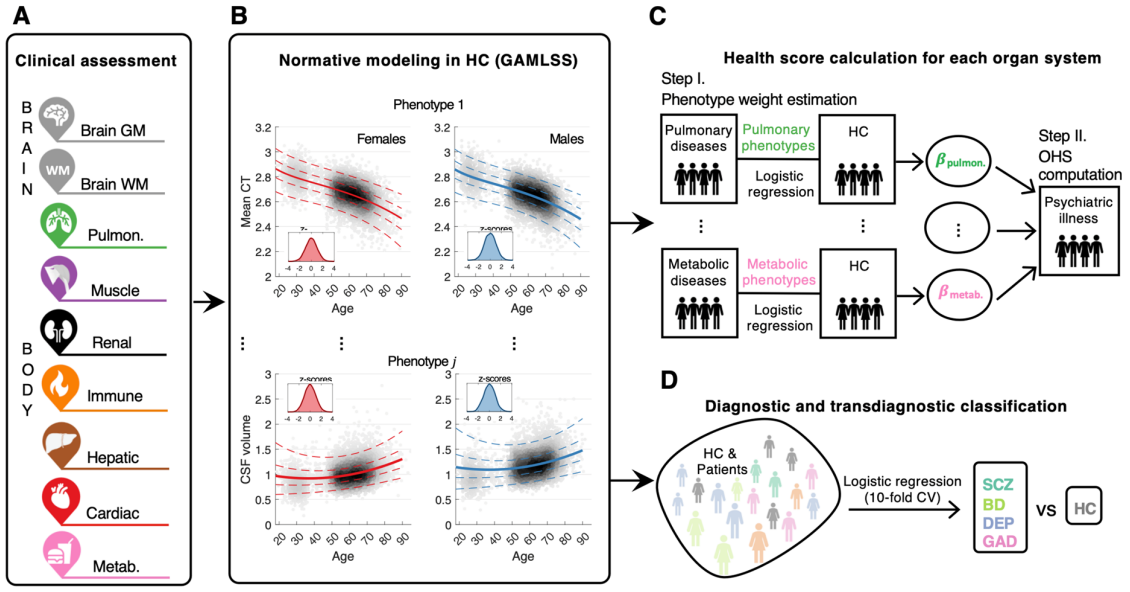

eFigure 1. Overview of study design. (**A**) Phenotypes derived from brain imaging, physical and physiological assessments were grouped into 2 brain and 7 body systems. (**B**) Normative age-related changes in each individual phenotype were established using generalized additive models for local, sale and shape (GAMLSS) in a group of healthy comparison (HC) individuals, stratified by sex. The median is denoted by a solid line. Dotted lines indicate 5%, 25%, 75% and 95% centiles (from bottom to top). The inset shows the distribution of the standardized phenotypic deviation scores (z-scores) across individuals. (**C**) Schematic of multi-system health profile mapping in individuals with neuropsychiatric disorders. An organ/system health score (OHS) was computed for each organ system and for each individual using organ-specific phenotypic deviation scores. The color of each violin plot corresponds to the organ system icon shown in panel (A). (**D**) Schematic of diagnostic and transdiagnostic disease classification using logistic regression applied to organ-specific phenotypic deviation scores. GM, gray matter; WM, white matter; CT, cortical thickness; CSF, cerebrospinal fluid; Cardiac., cardiovascular; Pulmon., pulmonary; Muscle, musculoskeletal; Metab., metabolic; CV, cross-validation; SCZ, schizophrenia; BD, bipolar disorder; DEP, depression; GAD, generalized anxiety disorder.

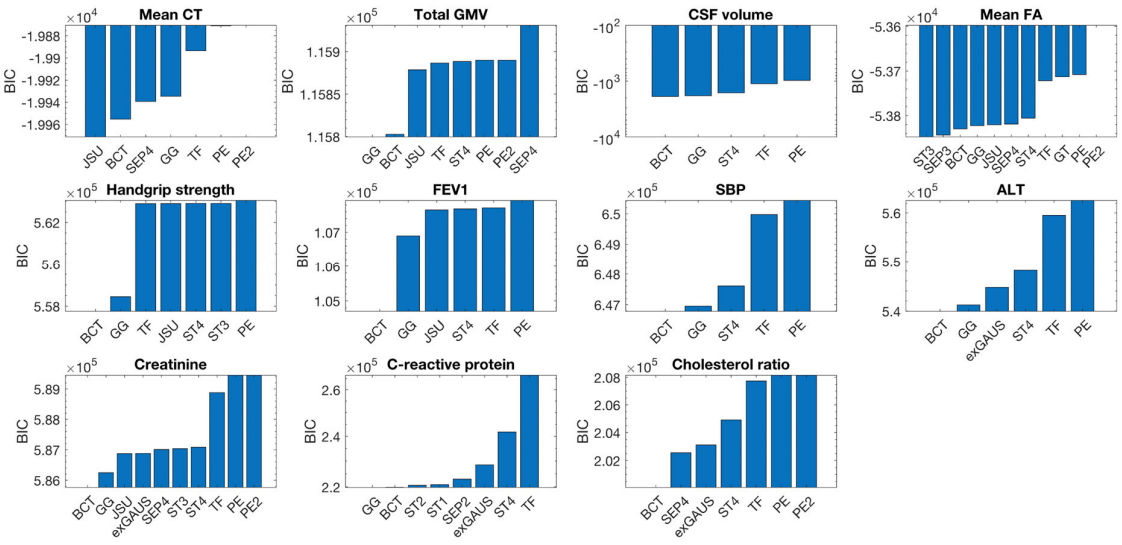

eFigure 2. Comparison of model distribution among converged GAMLSS models. The Bayesian information criterion (BIC) was computed for converged GAMLSS models for each representative brain and body phenotype. The Y-axis is shown in logarithmic scale to facilitate visualization. Models that did not converge were supressed from the plots. While the model with the lowest BIC varied across the 11 phenotypes, phenotypic variation was best modeled by the Box-Cox t (BCT) distribution overall. Distribution family acronyms are consistent with those listed in the GAMLSS package[26]. CT, cortical thickness; GMV, gray matter volume; CSF, cerebrospinal fluid; FA, fractional anisotropy; FEV1, forced expiration volume in 1-second; SBP, systolic blood pressure; ALT, serum alanine aminotransferase.

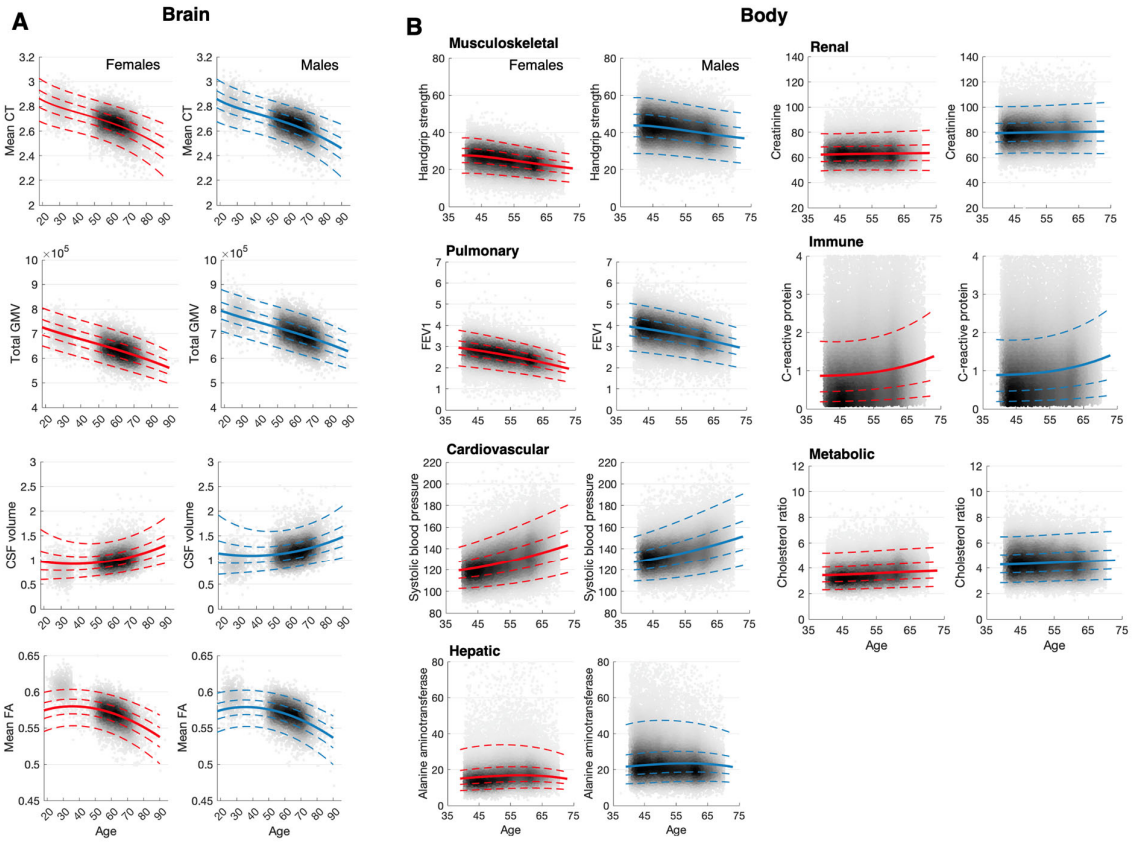

eFigure 3. **Examples of GAMLSS models for age-related trajectories in healthy individuals.** (**A**) Global brain phenotypes, including mean cortical thickness (CT), total gray matter volume (GMV), cerebrospinal fluid (CSF) volume and mean fractional anisotropy (FA). (**B**) Representative body phenotypes for 7 body systems, including the handgrip strength, forced expiration volume in 1-second (FEV1), systolic blood pressure, serum alanine aminotransferase, serum creatine, C-reactive protein and total-to-HDL cholesterol ratio. Models are shown for females (red) and males (blue) separately. The median is denoted as a solid line, whereas doted lines indicate 5%, 25%, 75% and 95% centiles (from bottom to top).

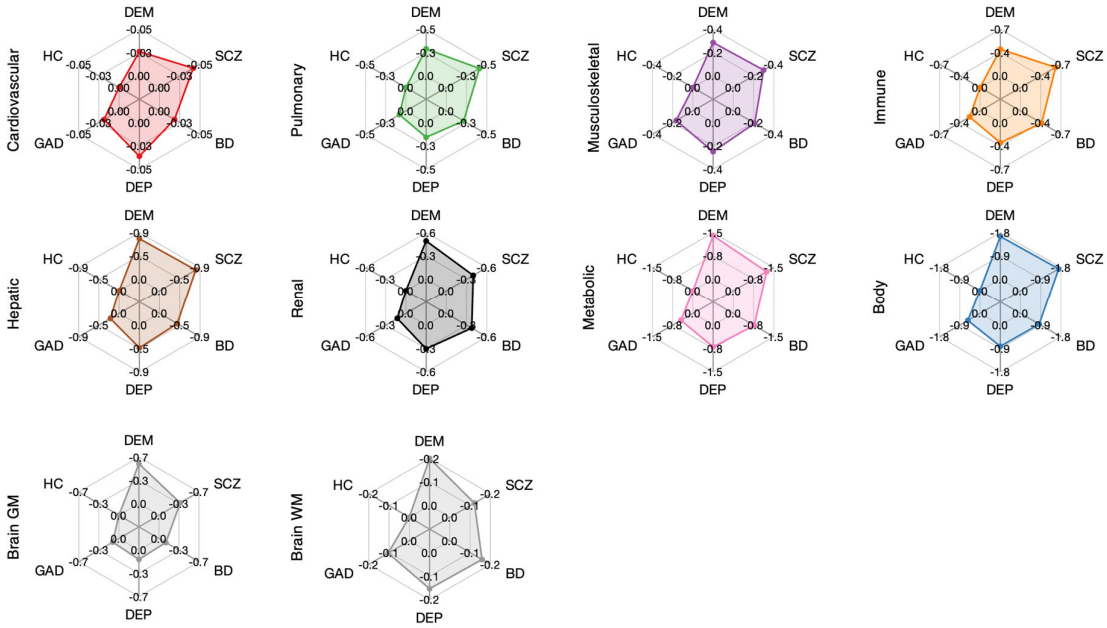

eFigure 4. Brain and body health scores in neuropsychiatric disorders stratified by organ system. Radial plots show the mean of estimated organ health scores within each neuropsychiatric disorder. Organ systems in each plot were organized anti-clockwise according to the mean health score, from the smallest to the largest value. GM, gray matter; WM, white matter; Cardiac, cardiovascular; Muscle, musculoskeletal; Pulmon., pulmonary; Metab., metabolic; DEM, dementia; SCZ, schizophrenia; BD, bipolar disorder; DEP, depression; GAD, generalized anxiety disorder; HC, healthy comparison.

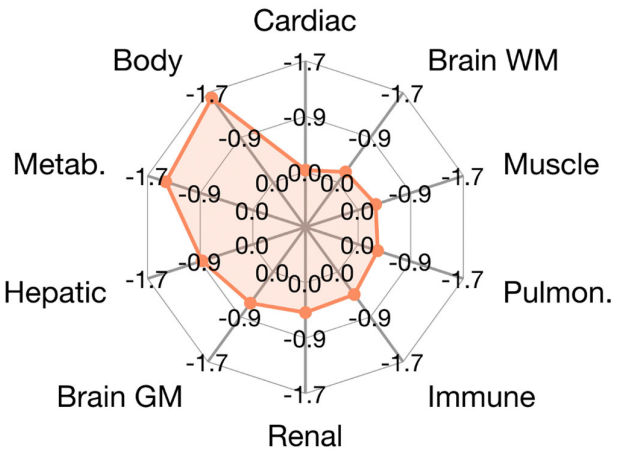

eFigure 5. Brain and body health scores in dementia. Radial plots show the mean of estimated organ health scores across individuals within dementia group. Organ systems were organized anti-clockwise according to the mean health score, from the smallest to the largest value. GM, gray matter; WM, white matter; Cardiac, cardiovascular; Muscle, musculoskeletal; Pulmon., pulmonary; Metab., metabolic; DEM, dementia.

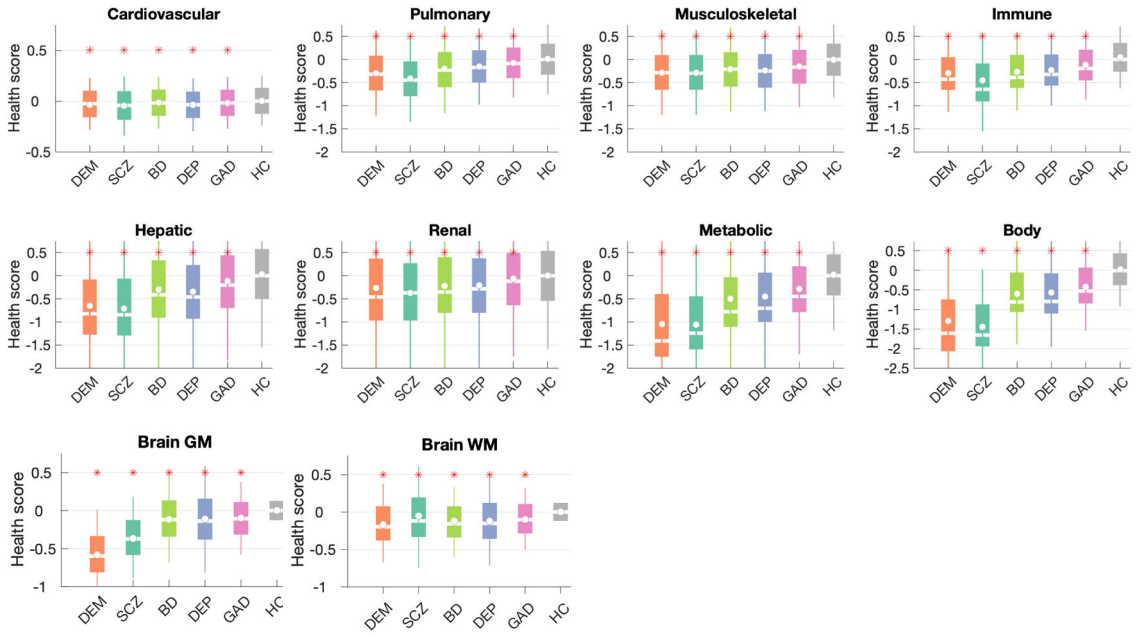

eFigure 6. Distribution of brain and body health scores in neuropsychiatric disorders stratified by organ system. Box plots in each panel show the distribution of estimated organ/system health scores across individuals within each neuropsychiatric disorder and healthy comparison (HC) individuals. An overall body health score was estimated using all body phenotypes (top right). A score of zero indicates healthy/normal organ function and scores below zero suggest deterioration of organ health, controlling for age and sex. Disease groups with significantly lower organ/system health scores than HC are marked with red asterisks (p<0.05, two-tailed, FDR corrected across 5 disorder groups x 10 organ systems=50 tests). Central line/circle mark on each box plot indicates the mean/median value. The bottom and top edges of each box plot indicate 40th and 60th percentiles of the distribution. The whiskers extend to the most extreme data points that are not considered outliers (1.5-times the interquartile range). GM, gray matter; WM, white matter; SCZ, schizophrenia; BD, bipolar disorder; DEP, depression; GAD, generalized anxiety disorder; DEM, dementia.

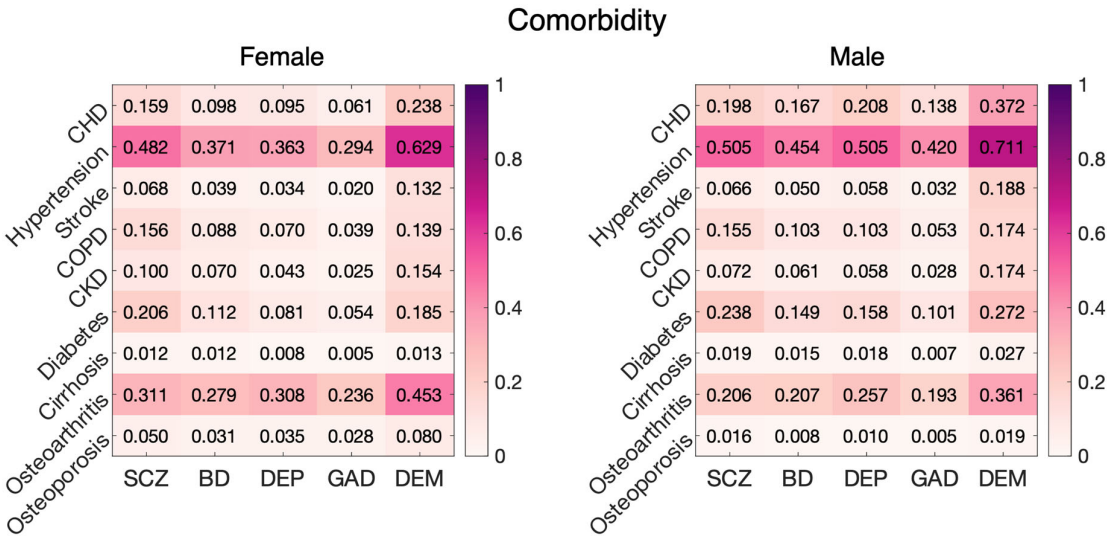

eFigure 7. Physical comorbidity rates. Proportions of female (left) and male (right) individuals with comorbid physical illness in individuals diagnosed with each of the five neuropsychiatric disorders in the UK Biobank cohort. SCZ, schizophrenia; BD, bipolar disorder; DEP, depression; GAD, generalized anxiety disorder; DEM, dementia. CHD, coronary heart disease; COPD, chronic obstructive pulmonary disease; CKD, chronic kidney disease.

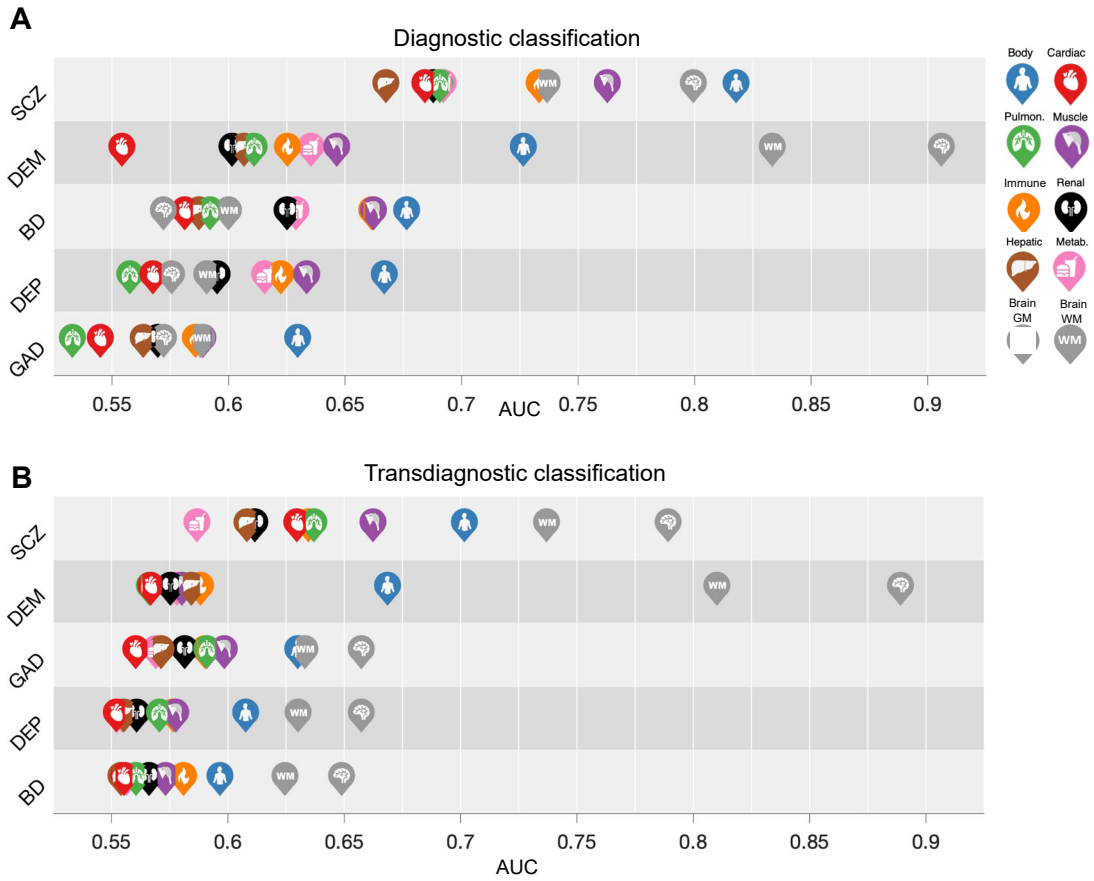

eFigure 8. Accuracy of diagnostic and transdiagnostic disease classification. (**A**) A logistic regression model was trained to classify an individual's diagnostic status (disease *X* vs HC). Classification models were established for each organ system, using organ-specific phenotypic deviation scores. Each row represents one target disease group *X,* where icons are positioned to indicate the model accuracy, as quantified by the area under the curve (AUC) of the receiver operating characteristic curve. (**B**) Similar to panel (A), but a logistic regression model was trained to classify an individual's diagnostic status between disease pairs (disease *X* vs disease *Y*). Each row represents one target disease group *X*, where icons are positioned to the average accuracy in differentiating disease group *X* from all the other groups. SCZ, schizophrenia; BD, bipolar disorder; DEP, depression; GAD, generalized anxiety disorder; DEM, dementia.

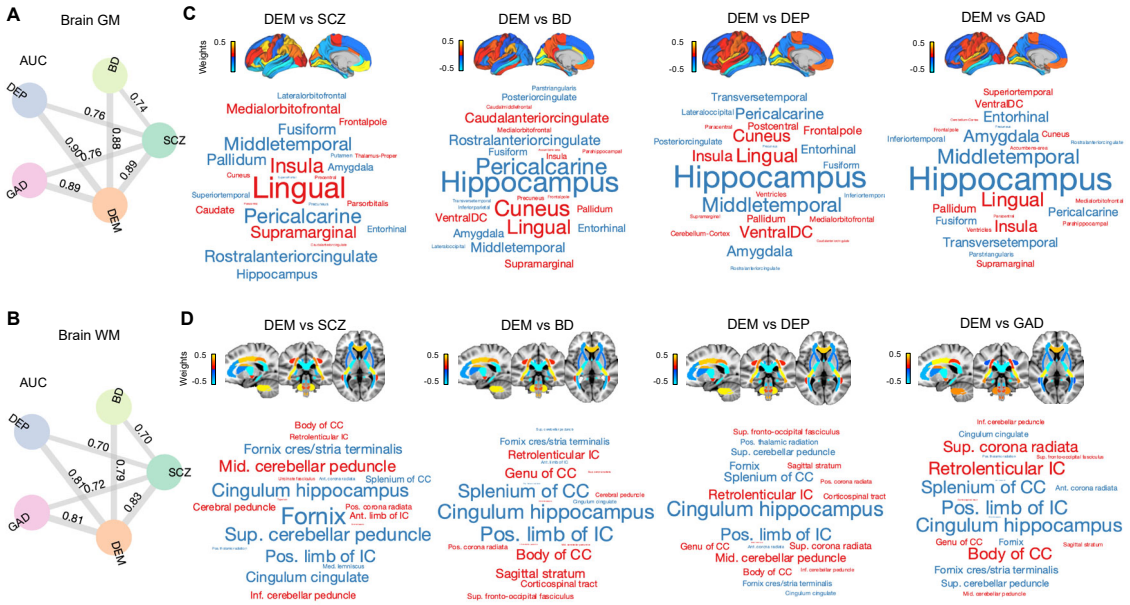

eFigure 9. Pairwise transdiagnostic disease classification and feature weights. Accuracy of disease classification using brain gray matter (GM, **A**) and white matter (WM, **B**) phenotypes for each pair of disorder groups. Each node represents one disease group. Edge thickness is modulated by the accuracy of disease classification between the two linked groups, as quantified by the area under the curve (AUC). Solid lines indicate models that significantly exceed chance-level accuracy intervals (permutation testing, n=1000, p<0.05, one-tailed, FDR corrected across 10 disease pairs). Non-significant accuracies are suppressed from the graph. (**C**) Regional gray matter features differentiating individuals with dementia from the other four neuropsychiatric disorders. Feature weights for cortical gray matter volume (Desikan-Killiany atlas) are rendered on cortical surface for visualization. Word clouds show top-ranked features including cortical and subcortical regions. The font color indicates weight polarity (red, positive; blue, negative). The font size is scaled according to the absolute weight of the feature. (**D**) Regional white matter features differentiating individuals with dementia from the other four neuropsychiatric disorders. Feature weights for regional fractional anisotropy (JHU ICBM-DTI-81 atlas). are rendered in anatomical space. Word clouds show top-ranked white matter tracts. The font color indicates weight polarity (red, positive; blue, negative). The font size is scaled according to the absolute weight of the feature. SCZ, schizophrenia; BD, bipolar disorder; DEP, depression; GAD, generalized anxiety disorder; DEM, dementia.

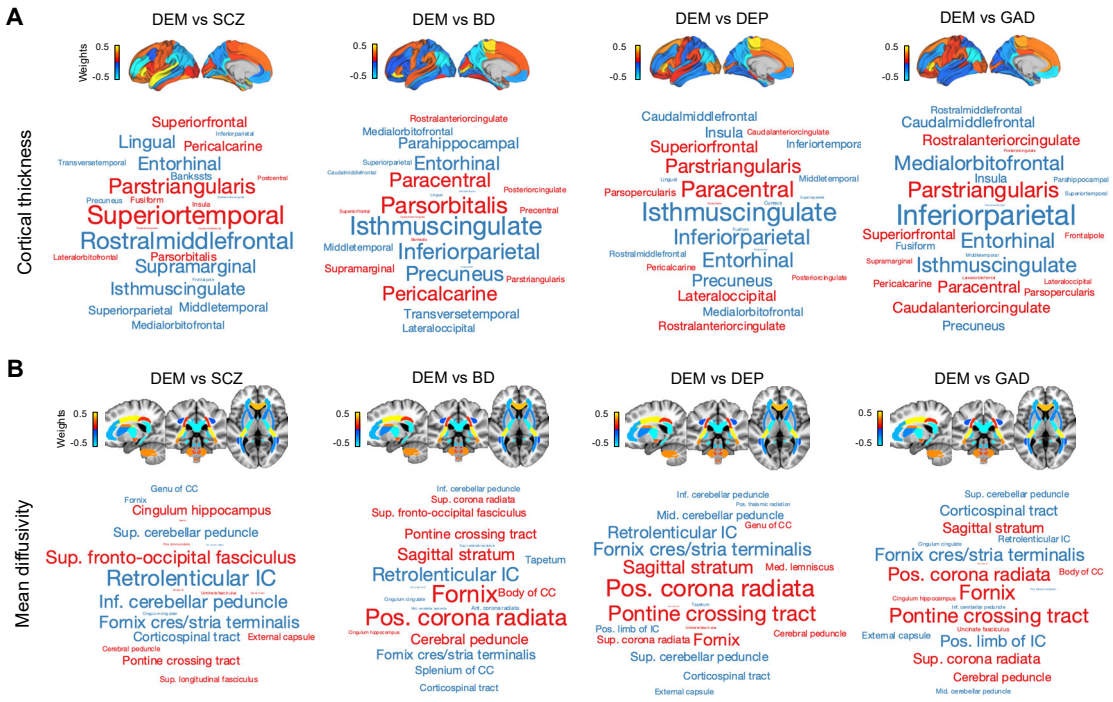

eFigure 10. Feature weights differentiating individuals with dementia from other neuropsychiatric disorders. (**A**) Feature weights for regional cortical thickness (Desikan-Killiany atlas) rendered on cortical surface for visualization. Word clouds show top-ranked features including cortical regions. The font color indicates weight polarity (red, positive; blue, negative). The font size is scaled according to the absolute weight of the feature. (**B**) Feature weights for regional diffusivity (JHU ICBM-DTI-81 atlas) rendered in anatomical space. The font color indicates weight polarity (red, positive; blue, negative). The font size is scaled according to the absolute weight of the feature. SCZ, schizophrenia; BD, bipolar disorder; DEP, depression; GAD, generalized anxiety disorder; DEM, dementia.

eTable 1. Brain gray matter phenotypes

Gray matter volume	Cortical thickness
Volume of bankssts	Mean thickness of bankssts
Volume of caudalanteriorcingulate	Mean thickness of caudalanteriorcingulate
Volume of caudalmiddlefrontal	Mean thickness of caudalmiddlefrontal
Volume of cuneus	Mean thickness of cuneus
Volume of entorhinal	Mean thickness of entorhinal
Volume of fusiform	Mean thickness of fusiform
Volume of inferiorparietal	Mean thickness of inferiorparietal
Volume of isthmuscingulate	Mean thickness of inferiortemporal
Volume of lateraloccipital	Mean thickness of isthmuscingulate
Volume of lateralorbitofrontal	Mean thickness of lateraloccipital
Volume of lingual	Mean thickness of lateralorbitofrontal
Volume of medialorbitofrontal	Mean thickness of lingual
Volume of middletemporal	Mean thickness of medialorbitofrontal
Volume of parahippocampal	Mean thickness of middletemporal
Volume of paracentral	Mean thickness of parahippocampal
Volume of parsopercularis	Mean thickness of paracentral
Volume of parsorbitalis	Mean thickness of parsopercularis
Volume of inferiortemporal	Mean thickness of parsorbitalis
Volume of parstriangularis	Mean thickness of parstriangularis
Volume of pericalcarine	Mean thickness of pericalcarine
Volume of postcentral	Mean thickness of posteriorcingulate
Volume of posteriorcingulate	Mean thickness of precentral
Volume of precentral	Mean thickness of precuneus
Volume of precuneus	Mean thickness of rostralanteriorcingulate
Volume of rostralanteriorcingulate	Mean thickness of rostralmiddlefrontal
Volume of rostralmiddlefrontal	Mean thickness of postcentral
Volume of superiorfrontal	Mean thickness of superiorfrontal
Volume of superiorparietal	Mean thickness of superiorparietal
Volume of superiortemporal	Mean thickness of superiortemporal
Volume of supramarginal	Mean thickness of supramarginal
Volume of frontalpole	Mean thickness of frontalpole
Volume of transversetemporal	Mean thickness of transversetemporal
Volume of insula	Mean thickness of insula
Volume of Cerebellum-Cortex	
Volume of Thalamus-Proper	
Volume of Caudate	
Volume of Putamen	
Volume of Pallidum	
Volume of Hippocampus	
Volume of Amygdala	

Volume of Accumbens-area
Volume of VentralDC
Volume of CSF

eTable 2. Brain white matter phenotypes

Fractional anisotropy (FA)	Mean diffusivity (MD)
Mean FA in middle cerebellar peduncle on FA skeleton	Mean MD in middle cerebellar peduncle on FA skeleton
Mean FA in pontine crossing tract on FA skeleton	Mean MD in pontine crossing tract on FA skeleton
Mean FA in genu of corpus callosum on FA skeleton	Mean MD in genu of corpus callosum on FA skeleton
Mean FA in body of corpus callosum on FA skeleton	Mean MD in body of corpus callosum on FA skeleton
Mean FA in splenium of corpus callosum on FA skeleton	Mean MD in splenium of corpus callosum on FA skeleton
Mean FA in fornix on FA skeleton	Mean MD in fornix on FA skeleton
Mean FA in corticospinal tract on FA skeleton	Mean MD in corticospinal tract on FA skeleton
Mean FA in medial lemniscus on FA skeleton	Mean MD in medial lemniscus on FA skeleton
Mean FA in inferior cerebellar peduncle on FA skeleton	Mean MD in inferior cerebellar peduncle on FA skeleton
Mean FA in superior cerebellar peduncle on FA skeleton	Mean MD in superior cerebellar peduncle on FA skeleton
Mean FA in cerebral peduncle on FA skeleton	Mean MD in cerebral peduncle on FA skeleton
Mean FA in anterior limb of internal capsule on FA skeleton	Mean MD in anterior limb of internal capsule on FA skeleton
Mean FA in posterior limb of internal capsule on FA skeleton	Mean MD in posterior limb of internal capsule on FA skeleton
Mean FA in retrolenticular part of internal capsule on FA skeleton	Mean MD in retrolenticular part of internal capsule on FA skeleton
Mean FA in anterior corona radiata on FA skeleton	Mean MD in anterior corona radiata on FA skeleton
Mean FA in superior corona radiata on FA skeleton	Mean MD in superior corona radiata on FA skeleton
Mean FA in posterior corona radiata on FA skeleton	Mean MD in posterior corona radiata on FA skeleton
Mean FA in posterior thalamic radiation on FA skeleton	Mean MD in posterior thalamic radiation on FA skeleton
Mean FA in sagittal stratum on FA skeleton	Mean MD in sagittal stratum on FA skeleton
Mean FA in external capsule on FA skeleton	Mean MD in external capsule on FA skeleton
Mean FA in cingulum cingulate gyrus on FA skeleton	Mean MD in cingulum cingulate gyrus on FA skeleton
Mean FA in cingulum hippocampus on FA skeleton	Mean MD in cingulum hippocampus on FA skeleton
Mean FA in fornix cres+stria terminalis on FA skeleton	Mean MD in fornix cres+stria terminalis on FA skeleton
Mean FA in superior longitudinal fasciculus on FA skeleton	Mean MD in superior longitudinal fasciculus on FA skeleton
Mean FA in superior fronto-occipital fasciculus on FA skeleton	Mean MD in superior fronto-occipital fasciculus on FA skeleton
Mean FA in uncinate fasciculus on FA skeleton	Mean MD in uncinate fasciculus on FA skeleton
Mean FA in tapetum on FA skeleton	Mean MD in tapetum on FA skeleton

eTable 3. Body phenotypes.

Field ID	Variable name	Body system
Hand grip strength	Hand grip strength (average)	Musculoskeletal
102-0.0	Pulse rate, automated reading	Cardiovascular
3062-0.0	Forced vital capacity (FVC)	Pulmonary
3063-0.0	Forced expiratory volume in 1-second (FEV1)	Pulmonary
3064-0.0	Peak expiratory flow (PEF)	Pulmonary
4079-0.0	Diastolic blood pressure, automated reading	Cardiovascular
4080-0.0	Systolic blood pressure, automated reading	Cardiovascular
21001-0.0	Body mass index (BMI)	Musculoskeletal
30000-0.0	White blood cell (leukocyte) count	Immune
30010-0.0	Red blood cell (erythrocyte) count	Immune
30020-0.0	Haemoglobin concentration	Immune
30030-0.0	Haematocrit percentage	Immune
30040-0.0	Mean corpuscular volume	Immune
30050-0.0	Mean corpuscular haemoglobin	Immune
30060-0.0	Mean corpuscular haemoglobin concentration	Immune
30070-0.0	Red blood cell (erythrocyte) distribution width	Immune
30080-0.0	Platelet count	Immune
30090-0.0	Platelet crit	Immune
30100-0.0	Mean platelet (thrombocyte) volume	Immune
30110-0.0	Platelet distribution width	Immune
30120-0.0	Lymphocyte count	Immune
30130-0.0	Monocyte count	Immune
30140-0.0	Neutrophill count	Immune
30150-0.0	Eosinophill count	Immune
30160-0.0	Basophill count	Immune
30170-0.0	Nucleated red blood cell count	Immune
30180-0.0	Lymphocyte percentage	Immune
30190-0.0	Monocyte percentage	Immune
30200-0.0	Neutrophill percentage	Immune
30210-0.0	Eosinophill percentage	Immune
30220-0.0	Basophill percentage	Immune
30230-0.0	Nucleated red blood cell percentage	Immune
30240-0.0	Reticulocyte percentage	Immune
30250-0.0	Reticulocyte count	Immune
30260-0.0	Mean reticulocyte volume	Immune
30270-0.0	Mean sphered cell volume	Immune
30280-0.0	Immature reticulocyte fraction	Immune
30290-0.0	High light scatter reticulocyte percentage	Immune
30300-0.0	High light scatter reticulocyte count	Immune
30510-0.0	Creatinine (enzymatic) in urine	Renal
30520-0.0	Potassium in urine	Renal

30530-0.0	Sodium in urine	Renal
30600-0.0	Albumin	Renal, Hepatic
30610-0.0	Alkaline phosphatase	Musculoskeletal, Hepatic
30620-0.0	Alanine aminotransferase (ALT)	Hepatic
30630-0.0	Apolipoprotein A	Metabolic
30640-0.0	Apolipoprotein B	Metabolic
30650-0.0	Aspartate aminotransferase (AST)	Hepatic
30660-0.0	Direct bilirubin	Hepatic
30670-0.0	Urea	Renal
30680-0.0	Calcium	Musculoskeletal, Renal
30700-0.0	Creatinine	Renal
30710-0.0	C-reactive protein	Immune
30720-0.0	Cystatin C	Renal
30730-0.0	Gamma glutamyltransferase	Hepatic
30740-0.0	Glucose	Metabolic
30750-0.0	Glycated haemoglobin (HbA1c)	Metabolic
30760-0.0	HDL cholesterol	Metabolic
30770-0.0	IGF-1	Body
30780-0.0	LDL direct	Metabolic
30790-0.0	Lipoprotein A	Metabolic
30810-0.0	Phosphate	Musculoskeletal, Renal
30830-0.0	SHBG	Body
30840-0.0	Total bilirubin	Hepatic
30850-0.0	Testosterone	Body
30860-0.0	Total protein	Renal, Hepatic
30870-0.0	Triglycerides	Metabolic
30880-0.0	Urate	Renal
30890-0.0	Vitamin D	Musculoskeletal
FEV1-FVC ratio	FEV1-FVC ratio	Pulmonary
Waist-hip circumference ratio	Waist-hip circumference ratio	Musculoskeletal
Heel bone mineral density	Heel bone mineral density (average)	Musculoskeletal
Ankle spacing width	Ankle spacing width (average)	Musculoskeletal
Cholesterol ratio	Cholesterol ratio	Metabolic
21021-0.0	Arterial stiffness index	Cardiovascular

eTable 4. Disease categories used for the estimation of phenotype weights specific to each organ system.

Organ system	Number of patients	ICD-10 code	Code description
Cardiovascular	47,085	I10	Essential (primary) hypertension
		I11	Hypertensive heart disease
		I12	Hypertensive renal disease
		I13	Hypertensive heart and renal disease
		I15	Secondary hypertension
		I25	Chronic ischaemic heart disease
		I50	Heart failure
		I70	Atherosclerosis
Pulmonary	47,102	J41	Simple and mucopurulent chronic bronchitis
		J42	Unspecified chronic bronchitis
		J43	Emphysema
		J44	Other chronic obstructive pulmonary disease
		J45	Asthma
		J47	Bronchiectasis
Musculoskeletal	9,718	M60	Myositis
		M61	Calcification and ossification of muscle
		M62	Other disorders of muscle
		M63	Disorders of muscle in diseases classified elsewhere
		M80	Osteoporosis with pathological fracture
		M81	Osteoporosis without pathological fracture
		M82	Osteoporosis in diseases classified elsewhere
Immune	12,335	D55	Anaemia dut to enzyme disorders
		D56	Thalassaemia
		D57	Sickle-cell disorders
		D58	Other hereditary haemolytic anaemias
		D59	Acquired haemolytic anaemia
		D60	Acquired pure red cell aplasia [erythroblastopenia]
		D61	Other aplastic anaemia
		D63	Anaemia in chronic diseases classified elsewhere
		D64	Other anaemias
		D65	Disseminated intravascular coagulation [defibrination syndrome]
		D66	Hereditary factor viii deficiency
		D67	Hereditary factor ix deficiency
		D68	Other coagulation defects
		D69	Purpura and other haemorrhagic conditions
		D70	Agranulocytosis
		D71	Functional disorders of polymorphonuclear neutrophils
		D72	Other disorders of white blood cells
		D73	Diseases of spleen
		D74	Methaemoglobinaemia

		D75	Other diseases of blood and blood-forming organs
		D76	Certain diseases involving lymphoreticular tissue and reticulohistiocytic system
		D77	Other disorders of blood and blood-forming organs in diseases classified elsewhere
		D80	Immunodeficiency with predominantly antibody defects
		D81	Combined immunodeficiencies
		D82	Immunodeficiency associated with other major defects
		D83	Common variable immunodeficiency
		D84	Other immunodeficiencies
		D86	Sarcoidosis
		D89	Other disorders involving the immune mechanism, not elsewhere classified
Hepatic	947	K70	Alcoholic liver disease
		K72	Hepatic failure, not elsewhere classified
		K73	Chronic hepatitis, not elsewhere classified
		K74	Fibrosis and cirrhosis of liver
		K75	Other inflammatory liver diseases
		K76	Other diseases of liver
		K77	Liver disorders in diseases classified elsewhere
Renal	4,489	N18	Chronic renal failure
Metabolic	70,024	E10	Insulin-dependent diabetes mellitus
		E11	Non-insulin-dependent diabetes mellitus
		E12	Malnutrition-related diabetes mellitus
		E13	Other specified diabetes mellitus
		E14	Unspecified diabetes mellitus
		E78	Disorders of lipoprotein metabolism and other lipidaemias

eTable 5. Diagnostic codes of schizophrenia.

Code type	Code	Code description
UK Biobank Self Report	1289	Schizophrenia
ICD 9	295	Schizophrenic disorders
ICD 9	2950	Simple type
ICD 9	2951	Hebephrenic type
ICD 9	2952	Catatonic type
ICD 9	2953	Paranoid type
ICD 9	2954	Acute Schizophrenic episode
ICD 9	2955	Latent schizophrenia
ICD 9	2956	Residual schizophrenia
ICD 9	2957	Schizoaffective type
ICD 9	2958	Other specified types of schizophrenia
ICD 9	2959	Unspecified schizophrenia
ICD 9	297	Delusional disorders
ICD 9	2970	Paranoid state, simple
ICD 9	2971	Paranoia
ICD 9	2972	Paraphrenia
ICD 9	2973	Induced psychosis
ICD 9	2978	Other specified paranoid states
ICD 9	2979	Unspecified paranoid state
ICD 9	2983	Acute paranoid reaction
ICD 9	2984	Psychogenic paranoid psychosis
ICD 10	F20	Schizophrenia
ICD 10	F200	Paranoid schizophrenia
ICD 10	F201	Hebephrenic schizophrenia
ICD 10	F202	Catatonic schizophrenia
ICD 10	F203	Undifferentiated schizophrenia
ICD 10	F204	Post-schizophrenic depression
ICD 10	F205	Residual schizophrenia
ICD 10	F206	Simple schizophrenia
ICD 10	F208	Other schizophrenia
ICD 10	F209	Schizophrenia, unspecified
ICD 10	F21X	Schizotypal disorder
ICD 10	F22	Persistent delusional disorders
ICD 10	F220	Delusional disorder
ICD 10	F228	Other persistent delusional disorders
ICD 10	F229	Persistent delusional disorder, unspecified
ICD 10	F23	Acute and transient psychotic disorders
ICD 10	F230	Acute polymorphic psychotic disorder without symptoms of schizophrenia
ICD 10	F231	Acute polymorphic psychotic disorder with symptoms of schizophrenia
ICD 10	F232	Acute schizophrenia-like psychotic disorder
ICD 10	F233	Other acute predominantly delusional psychotic disorders
ICD 10	F238	Other acute and transient psychotic disorders
ICD 10	F239	Acute and transient psychotic disorder, unspecified
ICD 10	F24X	Induced delusional disorder

ICD 10	F25	Schizoaffective disorders
ICD 10	F250	Schizoaffective disorder, manic type
ICD 10	F251	Schizoaffective disorder, depressive type
ICD 10	F252	Schizoaffective disorder, mixed type
ICD 10	F258	Other schizoaffective disorders
ICD 10	F259	Schizoaffective disorder, unspecified
ICD 10	F28X	Other nonorganic psychotic disorders
ICD 10	F29X	Unspecified nonorganic psychosis

eTable 6. Diagnostic codes of depression.

Code type	Code	Code description
UK Biobank Self Report	1286	Depression
ICD 9	311	Depressive disorder, not elsewhere classified
ICD 9	3119	Depressive disorder, not elsewhere classified
ICD 10	F32	Depressive episode
ICD 10	F320	Mild depressive episode
ICD 10	F321	Moderate depressive episode
ICD 10	F322	Severe depressive episode without psychotic symptoms
ICD 10	F323	Severe depressive episode with psychotic symptoms
ICD 10	F328	Other depressive episodes
ICD 10	F329	Depressive episode, unspecified
ICD 10	F33	Recurrent depressive disorder
ICD 10	F330	Recurrent depressive disorder, current episode mild
ICD 10	F331	Recurrent depressive disorder, current episode moderate
ICD 10	F332	Recurrent depressive disorder, current episode severe without psychotic symptoms
ICD 10	F333	Recurrent depressive disorder, current episode severe with psychotic symptoms
ICD 10	F334	Recurrent depressive disorder, currently in remission
ICD 10	F338	Other recurrent depressive disorders
ICD 10	F339	Recurrent depressive disorder, unspecified

eTable 7. Diagnostic codes of bipolar disorder.

Code type	Code	Code description
UK Biobank Self Report	1291	Mania/bipolar disorder/manic depression
ICD 9	2960	Manic-depressive psychosis, manic type
ICD 9	2962	Manic-depressive psychosis, circular type but currently manic
ICD 9	2963	Major depressive disorder, recurrent episode
ICD 9	2964	Manic-depressive psychosis, circular type but currently depressed
ICD 9	2965	Manic-depressive psychosis, circular type, current condition not specified
ICD 10	F302	Mania with psychotic symptoms
ICD 10	F31	Bipolar affective disorder
ICD 10	F310	Bipolar affective disorder, current episode hypomanic
ICD 10	F311	Bipolar affective disorder, current episode manic without psychotic symptoms
ICD 10	F312	Bipolar affective disorder, current episode manic with psychotic symptoms
ICD 10	F313	Bipolar affective disorder, current episode mild or moderate depression
ICD 10	F314	Bipolar affective disorder, current episode severe depression without psychotic symptoms
ICD 10	F315	Bipolar affective disorder, current episode severe depression with psychotic symptoms
ICD 10	F316	Bipolar affective disorder, current episode mixed
ICD 10	F317	Bipolar affective disorder, currently in remission
ICD 10	F318	Other bipolar affective disorders
ICD 10	F319	Bipolar affective disorder, unspecified

eTable 8. Diagnostic codes of generalized anxiety disorder.

Code type	Code	Code description	Notes
UK Biobank Self Report	1287	Anixety/panic attacks	This is not necessarily GAD. Not included.
ICD 9	3000	Anxiety states	3000.02 is GAD but UKB does not have. Not included.
ICD 10	F411	Generalised anxiety disorder	Included

eTable 9. Diagnostic codes of dementia.

Code type	Code	Code description
UK Biobank Self Report	1263	Dementia/Alzheimers/Cognitive Impairment
ICD 9	2902	Senile dementia, depressed or paranoid type
ICD 9	2903	Senile dementia with acute confusional state
ICD 9	2904	Arteriosclerotic dementia
ICD 9	2912	Other alcoholic dementia
ICD 9	2941	Dementia in other conditions classified elsewhere
ICD 9	3310	Alzheimer's disease
ICD 9	3311	Pick's disease
ICD 9	3312	Senile degeneration of brain
ICD 9	3315	Creutzfeldt-Jakob disease
ICD 10	A810	Sporadic Creutzfeldt-Jakob disease
ICD 10	F00	Dementia in Alzheimer's disease
ICD 10	F000	Dementia in Alzheimer's disease with early onset
ICD 10	F001	Dementia in Alzheimer's disease with late onset
ICD 10	F002	Dementia in Alzheimer's disease, atypical or mixed type
ICD 10	F009	Dementia in Alzheimer's disease, unspecified
ICD 10	F01	Vascular dementia
ICD 10	F010	Vascular dementia of acute onset
ICD 10	F011	Multi-infarct dementia
ICD 10	F012	Subcortical vascular dementia
ICD 10	F013	Mixed cortical and sub-cortical vascular dementia
ICD 10	F018	Other vascular dementia
ICD 10	F019	Vascular dementia, unspecified
ICD 10	F02	Dementia in other diseases classified elsewhere
ICD 10	F020	Dementia in Picks disease
ICD 10	F021	Dementia in Creutzfeldt-Jacob disease
ICD 10	F022	Dementia in Huntington’s disease
ICD 10	F023	Dementia in Parkinson’s disease
ICD 10	F024	Dementia in HIV disease
ICD 10	F028	Dementia in other specified diseases classified elsewhere
ICD 10	F03	Unspecified dementia
ICD 10	F051	Delirium superimposed on dementia
ICD 10	F106	Mental and behavioural disorders due to use of alcohol - amnesic syndrome
ICD 10	G30	Alzheimer’s disease
ICD 10	G300	Alzheimer’s disease with early onset
ICD 10	G301	Alzheimer’s disease with late onset
ICD 10	G308	Other Alzheimer's disease
ICD 10	G309	Alzheimer's disease unspecified

ICD 10	G310	Circumscribed brain atrophy
ICD 10	G311	Senile degeneration of brain
ICD 10	G318	Other specified degenerative diseases of nervous system
ICD 10	I673	Binswanger's disease

References

1. Sudlow C, Gallacher J, Allen N, et al. UK Biobank: An open access resource for identifying the causes of a wide range of complex diseases of middle and old age. *PLOS Medicine.* 2015;12(3):e1001779.
2. Miller KL, Alfaro-Almagro F, Bangerter NK, et al. Multimodal population brain imaging in the UK Biobank prospective epidemiological study. *Nature neuroscience.* 2016;19(11):1523-1536.
3. Davis KAS, Cullen B, Adams M, et al. Indicators of mental disorders in UK Biobank-A comparison of approaches. *Int J Methods Psychiatr Res.* 2019;28(3):e1796.
4. Davis KAS, Coleman JRI, Adams M, et al. Mental health in UK Biobank – development, implementation and results from an online questionnaire completed by 157 366 participants: a reanalysis. *BJPsych Open.* 2020;6(2):e18.
5. Alfaro-Almagro F, Jenkinson M, Bangerter NK, et al. Image processing and Quality Control for the first 10,000 brain imaging datasets from UK Biobank. *NeuroImage.* 2018;166:400-424.
6. Fischl B, Salat DH, Busa E, et al. Whole brain segmentation: automated labeling of neuroanatomical structures in the human brain. *Neuron.* 2002;33(3):341-355.
7. Desikan RS, Segonne F, Fischl B, et al. An automated labeling system for subdividing the human cerebral cortex on MRI scans into gyral based regions of interest. *Neuroimage.* 2006;31(3):968-980.
8. Mori S, Oishi K, Jiang H, et al. Stereotaxic white matter atlas based on diffusion tensor imaging in an ICBM template. *Neuroimage.* 2008;40(2):570-582.
9. Smith SM, Jenkinson M, Johansen-Berg H, et al. Tract-based spatial statistics: voxelwise analysis of multi-subject diffusion data. *Neuroimage.* 2006;31(4):1487-1505.
10. Loughland C, Draganic D, McCabe K, et al. Australian Schizophrenia Research Bank: a database of comprehensive clinical, endophenotypic and genetic data for aetiological studies of schizophrenia. *Aust N Z J Psychiatry.* 2010;44(11):1029-1035.
11. Lv J, Di Biase M, Cash RFH, et al. Individual deviations from normative models of brain structure in a large cross-sectional schizophrenia cohort. *Molecular psychiatry.* 2020.
12. Ellis KA, Bush AI, Darby D, et al. The Australian Imaging, Biomarkers and Lifestyle (AIBL) study of aging: methodology and baseline characteristics of 1112 individuals recruited for a longitudinal study of Alzheimer's disease. *Int Psychogeriatr.* 2009;21(4):672-687.
13. Petersen RC, Aisen PS, Beckett LA, et al. Alzheimer's Disease Neuroimaging Initiative (ADNI): clinical characterization. *Neurology.* 2010;74(3):201-209.
14. Lupton MK, Robinson GA, Adam RJ, et al. A prospective cohort study of prodromal Alzheimer's disease: Prospective Imaging Study of Ageing: Genes, Brain and Behaviour (PISA). *Neuroimage Clin.* 2021;29:102527.
15. Van Essen DC, Smith SM, Barch DM, Behrens TEJ, Yacoub E, Ugurbil K. The WU-Minn Human Connectome Project: An overview. *NeuroImage.* 2013;80:62-79.
16. Bookheimer SY, Salat DH, Terpstra M, et al. The Lifespan Human Connectome Project in Aging: An overview. *Neuroimage.* 2019;185:335-348.
17. Glasser MF, Sotiropoulos SN, Wilson JA, et al. The minimal preprocessing pipelines for the Human Connectome Project. *Neuroimage.* 2013;80:105-124.

18. Dale AM, Fischl B, Sereno MI. Cortical surface-based analysis. I. Segmentation and surface reconstruction. *Neuroimage.* 1999;9(2):179-194.
19. Rosen AFG, Roalf DR, Ruparel K, et al. Quantitative assessment of structural image quality. *Neuroimage.* 2018;169:407-418.
20. Ling J, Merideth F, Caprihan A, Pena A, Teshiba T, Mayer AR. Head injury or head motion? Assessment and quantification of motion artifacts in diffusion tensor imaging studies. *Human brain mapping.* 2012;33(1):50-62.
21. Fortin J-P, Cullen N, Sheline YI, et al. Harmonization of cortical thickness measurements across scanners and sites. *NeuroImage.* 2018;167:104-120.
22. Fortin J-P, Parker D, Tunç B, et al. Harmonization of multi-site diffusion tensor imaging data. *NeuroImage.* 2017;161:149-170.
23. Thomopoulos SI, Nir TM, Villalon-Reina JE, et al. Diffusion MRI Metrics and their Relation to Dementia Severity: Effects of Harmonization Approaches. *medRxiv.* 2021:2021.2010.2004.21263994.
24. Stasinopoulos DM, Rigby RA. Generalized Additive Models for Location Scale and Shape (GAMLSS) in R. *Journal of Statistical Software.* 2007;23(7):1 - 46.
25. Rigby RA, Stasinopoulos DM. Generalized additive models for location, scale and shape. *Journal of the Royal Statistical Society: Series C (Applied Statistics).* 2005;54(3):507-554.
26. Rigby RA, Stasinopoulos, M.D., Heller, G.Z., & De Bastiani, F. *Distributions for Modeling Location, Scale, and Shape: Using GAMLSS in R.* New York: Chapman and Hall/CRC; 2019.
27. Marquand AF, Rezek I, Buitelaar J, Beckmann CF. Understanding Heterogeneity in Clinical Cohorts Using Normative Models: Beyond Case-Control Studies. *Biological psychiatry.* 2016;80(7):552-561.
28. Rutherford S, Kia SM, Wolfers T, et al. The normative modeling framework for computational psychiatry. *Nature Protocols.* 2022;17(7):1711-1734.
29. Dunn PK, Smyth GK. Randomized Quantile Residuals. *Journal of Computational and Graphical Statistics.* 1996;5(3):236-244.
30. Guidi J, Lucente M, Sonino N, Fava GA. Allostatic Load and Its Impact on Health: A Systematic Review. *Psychotherapy and Psychosomatics.* 2021;90(1):11-27.
31. Seeman TE, Singer BH, Rowe JW, Horwitz RI, McEwen BS. Price of adaptation--allostatic load and its health consequences. MacArthur studies of successful aging. *Arch Intern Med.* 1997;157(19):2259-2268.
32. Seeman TE, McEwen BS, Rowe JW, Singer BH. Allostatic load as a marker of cumulative biological risk: MacArthur studies of successful aging. *Proceedings of the National Academy of Sciences of the United States of America.* 2001;98(8):4770-4775.
33. McEwen BS, Stellar E. Stress and the individual. Mechanisms leading to disease. *Arch Intern Med.* 1993;153(18):2093-2101.